The Astrophysical Journal, 579:468–481, 2002 November 1


# A GENERAL THEORY OF CONNECTIVITY AND CURRENT SHEETS IN CORONAL MAGNETIC FIELDS ANCHORED TO DISCRETE SOURCES

D. W. Longcope
Department of Physics, Montana State University, Bozeman, MT 59717

and

I. Klapper
Department of Mathematical Sciences, Montana State University, Bozeman, MT 59717
*Received 2002 March 2; accepted 2002 July 10*

## ABSTRACT

A scheme is presented for mapping the connectivity of a potential magnetic field arising from an arbitrary distribution of discrete sources. The field lines interconnecting the sources are classified into $N_d$ domains, defining the field's connectivity. The number of domains is shown to depend on the number of sources and on the numbers of nulls and separators according to a simple relation. A class of nonpotential equilibria are then generated by minimizing magnetic energy subject to constraints on the flux of each domain. The resulting equilibria are current-free within each domain and contain singular currents along each of the field's separators.

*Subject headings:* MHD — Sun: corona — Sun: magnetic fields

## 1. INTRODUCTION

Solar observations have led to a basic picture of coronal activity as arising from the interaction between "systems" of magnetic flux. To illustrate this point, Sweet (1958) sketched an example of a coronal field rooted in four sunspots (two positive and two negative). Magnetic activity arises, he suggested, from reconnection along the single field line lying at the interface of the four resulting flux systems. Models studied since then have confirmed that such field lines, called *separators*, are the sites of kinematic magnetic reconnection in three dimensions (Greene 1988; Lau & Finn 1990). A separator is the generalization to three dimensions of a two-dimensional X-point. Since most two-dimensional theories show reconnection occurring at X-points, it is not surprising that generalizations of these theories predict reconnection at separators. It has been shown both analytically and through simulations that current sheets develop dynamically at separators (Longcope & Cowley 1996; Galsgaard, Priest, & Nordlund 2000), much as current sheets develop at two-dimensional X-points (Syrovatskii 1971; Biskamp 1986).

Recently, Longcope (2001) proposed a variational model for *flux-constrained* magnetic equilibria. This model enumerated topologically distinct systems of flux called *domains*, defined by the sources their field lines connect. Minimizing magnetic energy subject only to constraints on the flux within each domain leads to a class of equilibria. Flux constraints are inherently less restrictive than the more common constraints, known as line-tying, so flux-constrained equilibria have lower energy than a general force-free field. This property makes flux-constrained equilibria a useful tool for quantifying energies available in solar flares (Longcope & Silva 1998), X-ray bright points (Longcope & Kankelborg 2001), and quiet-Sun heating (Longcope & Kankelborg 1999).

Flux-constrained equilibria were shown by Longcope to be current-free in every domain and to contain current sheets localized to features known as isolating loops. Isolating loops were defined from a schematic of the domain connections (the domain graph); however, their definition is not unique. It was shown that for general two-dimensional potential fields every X-point is an isolating loop and that the nonuniqueness in their definition is irrelevant to the resulting equilibrium. For general three-dimensional fields it could be shown that separators form at least parts of isolating loops, but a similarly powerful statement could not be made. This left open two questions concerning the properties of flux-constrained equilibria as they might apply to a coronal field: (1) Will every separator in a given field contain a current sheet? (2) Will current sheets be found only at separators, or might there be other pieces in an isolating loop?

The difficulty in a general application stems from a poor understanding of the topologies possible in three-dimensional fields. Apart from the four-pole system introduced by Sweet and models of the Earth's magnetosphere, very few examples have been studied. Only in the past several years has an effort been made to catalog the possible connectivities between a handful of magnetic poles through a potential magnetic field (Bungey, Titov, & Priest 1996; Brown & Priest 2001).

There is a need for a general scheme for analyzing field topologies apart from the theory of flux-constrained equilibria. Over the past decade observations of solar flares have begun to be interpreted in terms of the magnetic field's three-dimensional topology (Démoulin et al. 1994; Bagalá et al. 1995; Aulanier et al. 2000; Fletcher et al. 2001). These analyses identify topologically significant features such as separatrices and separators, in a model magnetic field. At present there is no systematic procedure for identifying all of the separators and separatrices present in even a potential extrapolation. This deficiency can affect their use in any careful analysis.

This work presents a systematic scheme for characterizing the connectivity of the potential magnetic field generated by a set of sources. This requires the introduction of numerous new terms, whose definitions are repeated in an Appendix for the reader's convenience. General formulae are derived for the number of magnetic domains, $N_d$, and the structure of their domain graph. This general construction is used to

show that every isolating loop is composed only of separators and that every separator is part of at least one isolating loop. This provides a practical technique for calculating all domain fluxes in the potential field from a path integral along each separator. A class of flux-constrained fields follows from energy minimization while the domain fluxes are constrained to values different from the potential field. We further show that while the isolating loops can be chosen in several different ways, every choice leads to exactly the same flux-constrained equilibrium. This provides a definitive answer to the questions concerning flux-constrained fields: current sheets will occur only at separators, and every separator will have a current sheet. We conclude by applying the technique to an observed active region modeled using $N_s = 20$ magnetic sources.

## 2. THE POTENTIAL MAGNETIC FIELD

We first propose a scheme to completely characterize the connectivity of a potential magnetic field. To be as general as possible, we consider an unbounded three-dimensional volume excluding a countable set of isolated star-shaped regions, called *source regions*. Each source region is enclosed by a topologically spherical (i.e., genus-zero) surface, called the *source skin* $\partial\mathscr{R}$. In the case that point sources are used, the source skins will be infinitesimal spherical shells. To apply this general formulation to the solar corona, we will later assume that the source regions are flat and restricted to a plane (the photosphere) and we will consider only the magnetic field above this plane. Before returning to this special case, however, we will make no assumptions about the shape or distribution of source surfaces and will consider the field in the entire unbounded volume.

Within our volume we consider a magnetic field ($\nabla \cdot \boldsymbol{B} = 0$) that is current-free ($\nabla \times \boldsymbol{B} = 0$) and matches specified normal components $B_n$ on each source skin. The surface field $B_n$ will be finite and either positive or negative over an entire source. The field is the gradient of a harmonic potential, $\boldsymbol{B} = -\nabla\chi$, $\nabla^2\chi = 0$, which satisfies Neumann conditions on the source skins: $\partial\chi/\partial n = -B_n$.

The sources will be assigned unique indices denoted by variables $a$, $b$, or $c$. The total flux leaving source $a$ will be denoted

$$\Phi_a \equiv \oint_{\partial\mathscr{R}_a} B_n \, da \, . \tag{1}$$

If the complete set of sources has net flux $\sum_a \Phi_a \neq 0$, then we will include infinity as an additional source containing the balance of flux. In this way the net flux of all sources will always vanish. Hereafter, we will not distinguish between finite sources and the possible source at infinity.

With notable exceptions contained within a region of zero measure, elaborated below, every field line originates in a positive source and terminates in a negative source. Including infinity as a source makes this statement apply equally to "open" field lines. The volume is thus partitioned into $N_d$ *domains* defined by the pair of sources at the end of each field line such that all field lines within a given domain are *homotopic*, meaning that they may be continuously deformed into one another without leaving the domain. (Note that there may be multiple domains connecting the same two sources.) Between domains there must be boundary surfaces, called *separatrices*, which we will assume to be as smooth as needed. Since the normal flux $B_n$ never vanishes, there will be no "bald patches," and each separatrix in a generic potential magnetic field is the fan surface of a magnetic null point (Bungey et al. 1996).

A null point $\boldsymbol{x}_\alpha$ is a location where the magnetic field vector vanishes [$\boldsymbol{B}(\boldsymbol{x}_\alpha) = 0$]. In the neighborhood of this point the magnetic field can be approximated by its first nonvanishing term

$$\boldsymbol{B}(\boldsymbol{x}_\alpha + \delta\boldsymbol{x}) \simeq \mathbf{J}^\alpha \cdot \delta\boldsymbol{x} \, , \tag{2}$$

where $J^\alpha_{ij} = \partial B_i/\partial x_j$ is the Jacobian matrix evaluated at $\boldsymbol{x}_\alpha$. This matrix is symmetric and traceless owing to the conditions $\nabla \times \boldsymbol{B} = 0$ and $\nabla \cdot \boldsymbol{B} = 0$, respectively. The matrix therefore has three orthogonal eigenvectors and three real eigenvalues that sum to zero.

In general the null can be classified as either positive or negative depending on the sign of $-\det \mathbf{J}^\alpha$ (Yeh 1976; Parnell et al. 1996). The case $\det \mathbf{J}^\alpha = 0$ is not structurally stable; i.e., slight changes to the magnetic field would make $\det \mathbf{J} \neq 0$. We henceforth discount the possibility of such accidents.

A positive null (also called a B-type null in the literature) has two positive eigenvalues, whose eigenvectors define a surface called the local fan plane. Field lines within this plane originate at the null point, and their extension beyond the null's local neighborhood forms the full *fan surface*. Two *spine* field lines terminate in the null point, entering along the directions parallel and antiparallel to the third eigenvector, normal to the fan plane. The fan and spine field lines of a negative null point (or A-type null point) run in the opposite direction: they terminate and originate in the null point, respectively.

Fan and spine field lines are the only exceptions to our general contention that every field line belongs to one and only one domain. Closed or ergodic field lines are not present in a potential magnetic field. The fans and spines therefore form the boundaries between domains, together defining its *skeleton* (Priest, Bungey, & Titov 1997). A complete characterization of a field's connectivity follows from a complete characterization of its fans and spines.

## 3. CHARACTERIZING THE SKELETON

### 3.1. *Spine Sources*

The first step in a general characterization is to locate all of the null points of the potential field. In our general discussion, each of the nulls will be given a unique index denoted by the Greek variables $\alpha$, $\beta$, or $\gamma$. Negative and positive nulls will be denoted $A_\alpha$ and $B_\beta$, respectively.

We illustrate our general formulation with an example representing a possible coronal field. It is generated by six flat source regions of assorted fluxes arranged haphazardly on the $z = 0$ plane, as shown in Figure 1. The potential field contains four null points, all in the same plane as the sources ($z = 0$). These are two positive null points, $B_1$ and $B_2$, and two negative null points, $A_3$ and $A_4$.

The next step in the analysis is to trace both spine field lines from each null to their terminal sources.[1] The spines of a positive (negative) null terminate in positive (negative)

[1] Hereafter, we will not distinguish between tracing a field line in the direction parallel or antiparallel to $\boldsymbol{B}$; "forward" will mean away from the specified initial point.

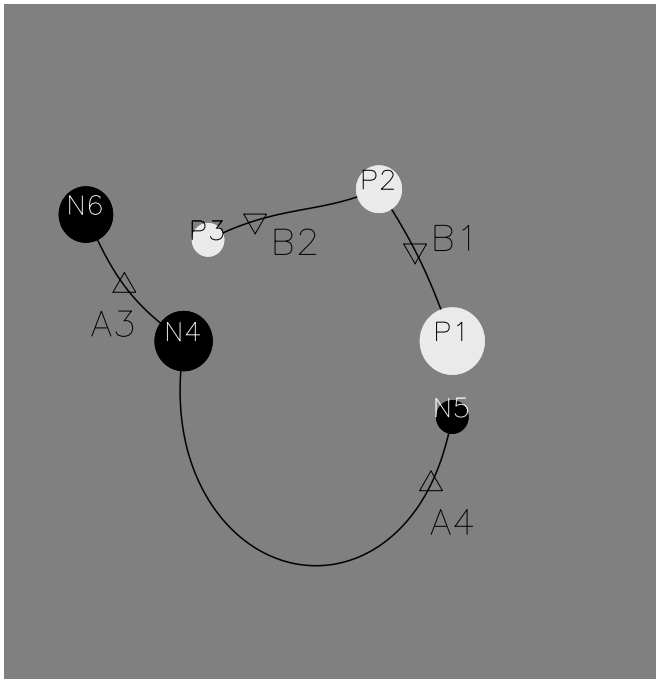


FIG. 1.—Six sources, arranged on the $z = 0$ plane, are represented as disks whose areas are proportional to their fluxes. Four nulls in the potential field, also located at $z = 0$, are shown with triangles. The spines from each null are shown as solid curves.

sources, called the *spine sources* of the null. The fan of a positive null, with spine sources $P_a$ and $P_b$, will separate domains originating in $P_a$ from domains originating in $P_b$. This follows from the fact that field lines in a neighborhood of the fan surface will end in either of the spine sources, depending on which side of the fan they occupy.

If both spines from a null terminate in the same source, then the fan surface makes no actual division between domains, and it is not part of the field's skeleton. We refer to these as *internal* nulls and consider them no further. If the two spines go to different sources, the fan surface is part of the field's skeleton, and this is a *boundary null*. Figure 1 shows the spine field lines (*solid lines*), demonstrating that all four nulls are boundary nulls.

### 3.2. *Fan Sectors*

Fan field lines leave a null in all directions in its fan plane, each terminating at a *fan source* of sign opposite to that of the spine source. If all of a fan's field lines go to the same source, it is an *unbroken* fan. An unbroken fan is, together with its null point and source, a closed topologically spherical surface dividing the full volume into two subvolumes containing the two spine sources. The fan source is the only source shared by domains in both volumes. Null $A_4$ in the example has an unbroken fan going to source $P_1$; its upper half is shown in green in Figure 2. This surface separates $N_5$ from $N_4$; in this case the domain $P_1$–$N_5$ is the only one inside the closed surface.

We will separately analyze each of the subvolumes defined by the unbroken fan. The exclusion of a star-shaped volume adjoining one of the source regions will not affect the connectivity of remaining volume. Once we have excluded all of these, no unbroken fans remain in the subvolume under consideration. Denote by $N_s$ and $N_0$ the numbers of sources and boundary nulls inside this subvolume. The fan of each null is *broken* into two or more *sectors*, according to the sources at its ends. Different sectors must lie in different domains and must therefore be separated by a separatrix surface. The single fan field line at the sector boundary must therefore belong simultaneously to a positive fan and a negative fan. It is a *separator field line* or null-null line, defined as the intersection of two fan surfaces.[2]

A negative null whose fan is divided into $n$ sectors must connect to $n$ positive nulls through $n$ different separators. Of the four separators linking $A_3$ to $B_1$ and $B_2$ the two above $z = 0$ are shown as magenta curves in Figure 3, while the other two are their mirror images below $z = 0$. Figure 4 is a schematic depiction of how these four separators divide the fan of $A_3$ into four sectors.

A sector from negative null $A_\alpha$ will consist of field lines terminating at this null and originating in a positive source

[2] In a potential field separatrix surfaces intersect along a curve that is therefore a field line. In more general fields they intersect along a ribbon of finite width.

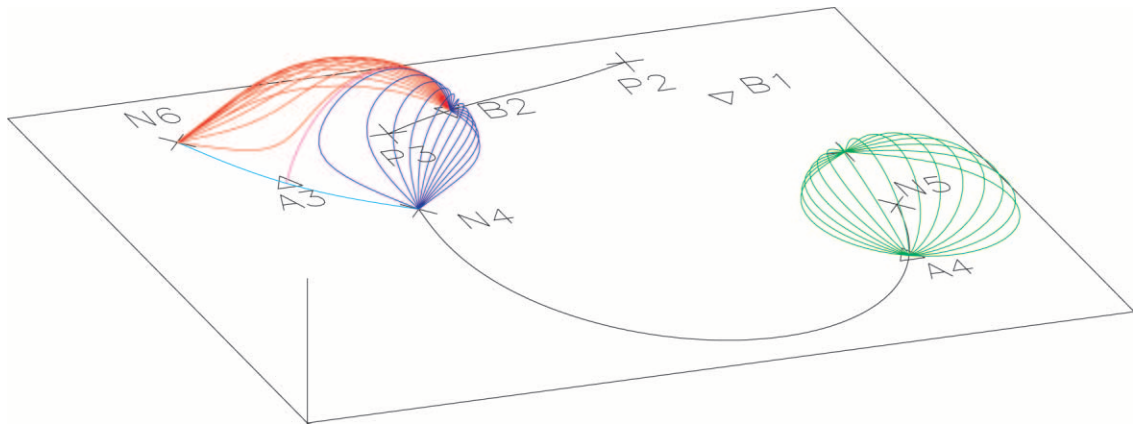


FIG. 2.—Fan field lines from nulls $B_2$ and $A_4$ in the upper half-space $z > 0$. The lower half-space is a mirror reflection of this. The fan from $A_4$ (*green*) is unbroken—all field lines go to $P_1$. The fan from $B_2$ consists of two sectors, one going to $N_4$ (*blue*) and the other to $N_6$ (*red*). One separator, going to $A_3$ (*magenta*), divides these sectors above the plane; a second separator is a mirror image of this below $z = 0$. The spines from $A_3$ are shown in cyan.

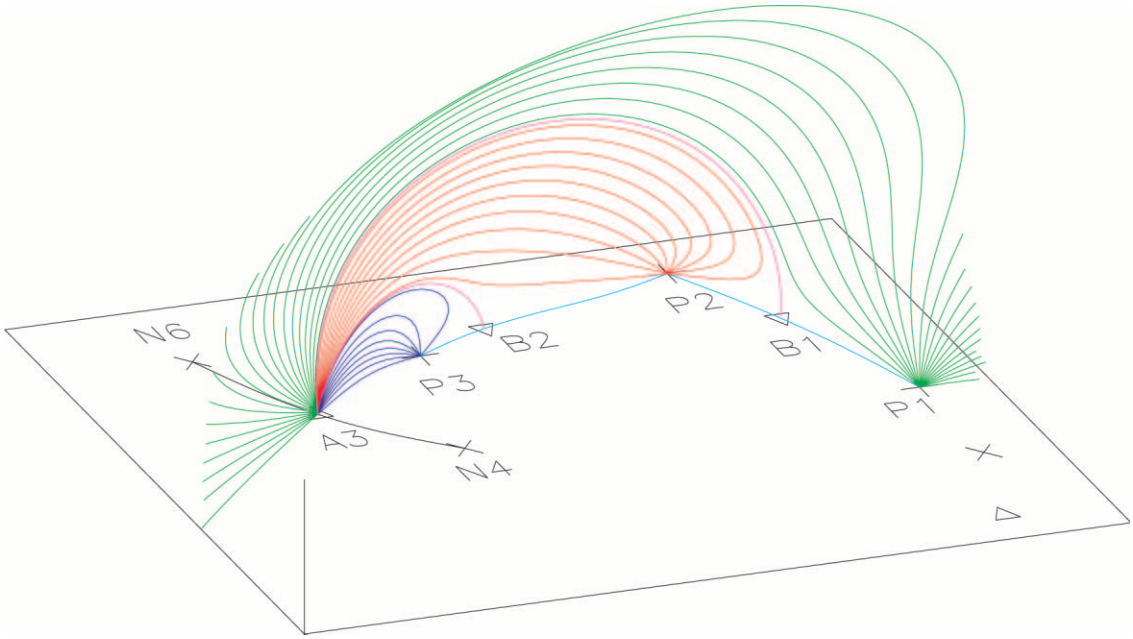


FIG. 3.—Fan field lines from null $A_3$ similar to Fig. 2. Field lines from three sectors are colored blue ($P_3$), red ($P_2$), and green ($P_1$). Only the upper portion of this sector is shown. The blue and green sectors continue below $z = 0$; a fourth sector located entirely within the lower half-space is a mirror image of the red sector. Separators dividing these sectors are shown in magenta, and the spines from the positive nulls are shown in cyan.

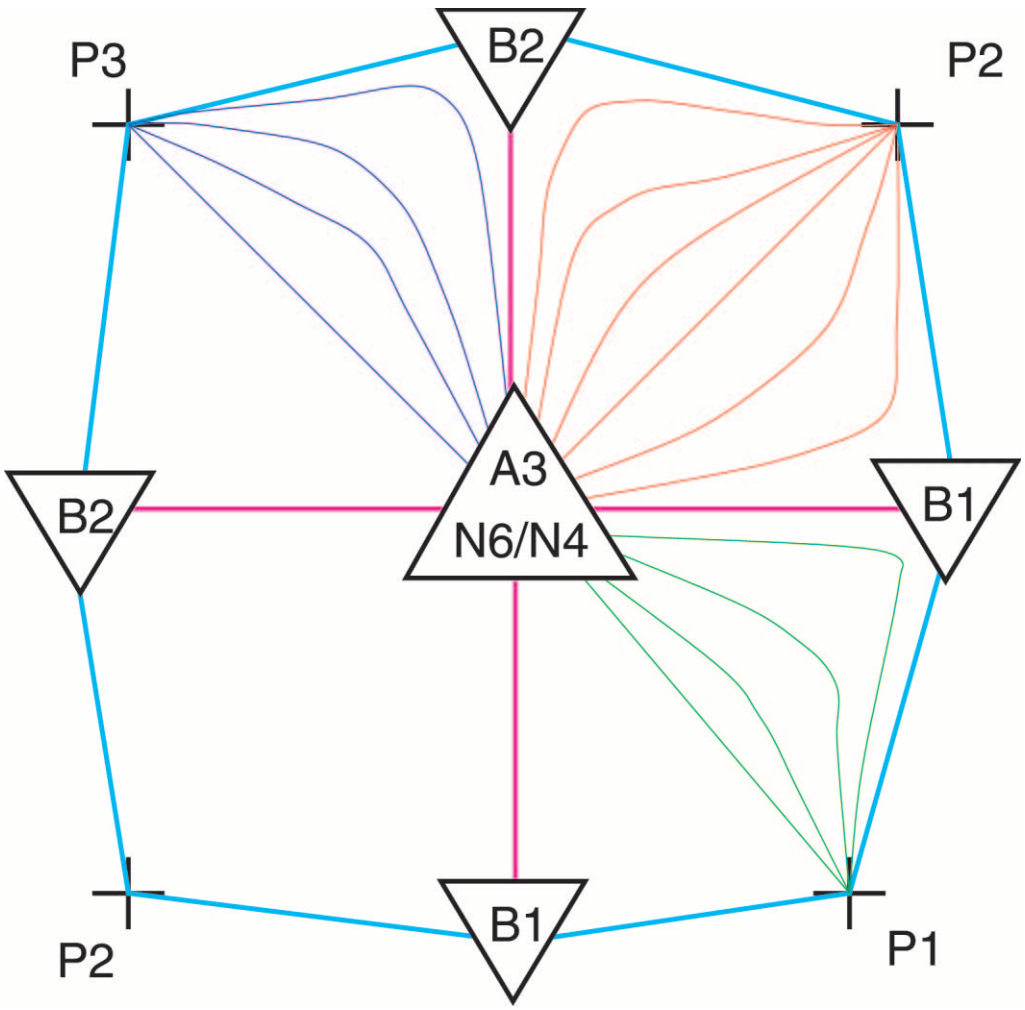


FIG. 4.—Schematic depiction of the fan surface from $A_3$; a perspective view of its upper half is shown in Fig. 3. Colored lines correspond to those shown in Fig. 3. Each of its four sectors is a quadrilateral bounded by 2 spines (*cyan*) and two separators (*magenta*).

$P_a$. It is bounded on two sides by separators $S_\rho$ and $S_\sigma$ connecting $A_\alpha$ to opposing nulls $B_\beta$ and $B_\gamma$. It is possible for $B_\beta = B_\gamma$, but for the fan to be truly broken $S_\rho \neq S_\sigma$. One spine from each of the nulls $B_\beta$ and $B_\gamma$ goes to $P_a$. These form the other two edges of the sector. If $B_\beta = B_\gamma$, then these are the same spine, as in the blue sector in Figure 3. Even in these cases we will count the single spine as two distinct edges of the sector. Thus, each sector is a deformed quadrilateral with edges being two separators and two spines. Its vertices are three nulls and one source. The fan surface is a union of sectors, and our analysis of domain boundaries will follow from an analysis of all sectors.

### 3.3. *The Domain Structure*

The entire structure of flux domains, sectors, separators and spines, and nulls and sources comprise a *CW complex* (Munkres 1984). It is then possible to determine the number of flux domains using Euler's relation $c - f + e - v = 0$ describing the partition of space into $c$ cells (domains), $f$ faces (sectors), $e$ edges (separators and spines), and $v$ vertices (nulls and sources). The total number of sectors includes those in positive fans and those in negative fans. In each fan the number of sectors is equal to the number of separators connecting to the null. Thus, the total number of sectors in positive fans equals the total number of separators leaving positive nulls. Similarly, the total number of sectors in negative fans equals the total number of separators leaving negative nulls. Every separator connects one positive null to one negative null, so the number of separators leaving each type of null is equal. Therefore, the total number of sectors $f = 2N_{\rm nn}$ is twice the number of separators $N_{\rm nn}$.

Every spine and every separator is an edge of at least one sector. The first fact follows because every null must be connected to at least two separators (lest its fan be unbroken). Each separator lies at the edge of four sectors, two of which will have the null's spines at its edge. Thus, every spine is an edge to two or more sectors. The second fact follows from the observation that every separator, being the intersection of two fan surfaces, is generically an edge to four sectors. Since every null has exactly two spines, the total number of spines is twice $N_0$, the number of nulls with sectored fans within the subvolume under consideration. This means that the total number of edges, $e$, is the total number of separators plus the total number of spines: $e = N_{\rm nn} + 2N_0$.

Within the subvolume being considered, every source and every null is a vertex. Since every source belongs to at least two domains, it connects to at least one sector. Every null is the vertex of at least six sectors. Thus, the total number of vertices is the total number of nulls plus the total number of sources: $v = N_0 + N_s$.

Euler's relation states $c = f - e + v$, which in turn implies

$$N_d = N_{\rm nn} - N_0 + N_s \ , \tag{3}$$

where $N_d =$ the number of flux domains. In the example, $N_s = 5$ (excluding source $N_5$), $N_0 = 3$ (excluding null $A_4$), and $N_{\rm nn} = 4$ (including reflection in $z < 0$). This leads to $N_d = 6$ domains. We will identify all of these domains below.

The best way to identify domains is to consider how sectors divide up the flux from each source. Field lines leave a given source $P_a$ in all directions, forming a topological ball. Field lines from a given domain make up a double cone of this ball with endpoints at each source of the domain. The faces of this cone are made up of sectors. A domain connecting source $P_a$ to $N_b$ must be bounded by both positive and negative sectors. The negative sectors form a cone with $P_a$ at its apex; the positive sectors form a cone with $N_b$ at its apex. The two cones join along a closed curve consisting of separators—separators are where positive and negative fan surfaces intersect. Therefore, each flux domain is ringed by exactly one closed curve of separators, or *separator circuit*.

To enumerate all possible separator circuits, we construct a *null graph* whose vertices are the nulls and whose edges are separators connecting pairs of nulls. In general, more than one edge can connect a pair of vertices, making the construction a *multigraph* in the terminology of graph theory. We adopt the convention that edges incident on a vertex are to be drawn in the order in which they occur within the fan. We also notate the source connected by each fan sector appearing between edges. With the sectors indicated this way we call this a labeled null graph.

A domain connecting $P_a$ to $N_b$ corresponds to a unique circuit in the null graph. This circuit appears within that subgraph that includes only nulls for which $P_a$ and $N_b$ are spine sources. In order for the circuit to pass from edge $S_\sigma$ to edge $S_\rho$, they must be incident on vertex $A_\alpha$ with only the fan source $P_a$ between them. Similarly, consecutive edges must be incident on a negative vertex $B_\beta$ with only the fan source $N_b$ between them.

Figure 5, for example, shows the circuit corresponding to domain $\mathscr{D}_3$, linking $P_2$ and $N_4$, to be

$$A_3 \rightarrow S_1 \rightarrow B_1 \rightarrow S_3 \rightarrow A_3 \rightarrow S_4 \rightarrow B_2 \rightarrow S_2 \rightarrow A_3 \ .$$

This same circuit can also be seen to enclose $\mathscr{D}_4$ linking $P_2$ to $N_6$, so the association between null circuits and domains is not one to one. While every domain corresponds to a unique separator circuit, a given circuit might correspond to several domains. We elaborate on this relation further below.

From the labeled null graph it is possible, using the rule above, to build up the domain graph depicting all domains and the sources they link. For a given pair of opposing sources, $P_a$ and $N_b$, first extract the subgraph of nulls whose spine sources include $P_a$ or $N_b$. Then identify all circuits in this subgraph whose consecutive edges enclose either fan source $P_a$ or $N_b$. Each such circuit corresponds to a different domain, which is then added to the domain graph. Once this has been done for each and every pair of opposite sources, the domain graph is complete. The null graph (Fig. 5, *left panel*) generates the six domains shown in the right panel of Figure 5. In this case there is one and only one domain connecting each opposing pair.

The general method of translating labeled null graphs to domain graphs is demonstrated by applying it to a few more simple cases. In all, there are four possible connected null graphs having four edges or fewer, of which the left panel of Figure 5 is one. The other three possibilities are shown in Figure 6, along with the corresponding domain graphs. Labeling is unnecessary since all possibilities are equivalent in these simple graphs. The simplest, denoted (i), corresponds to "Sweet's configuration" with four sources and two nulls (Sweet 1958; Gorbachev & Somov 1988). In a coronal arrangement (described further in § 6) the nulls lie on the source plane, $z = 0$, and are connected by a single separator above and its mirror image below. A second null graph, denoted (iii), corresponds to the same domain graph.

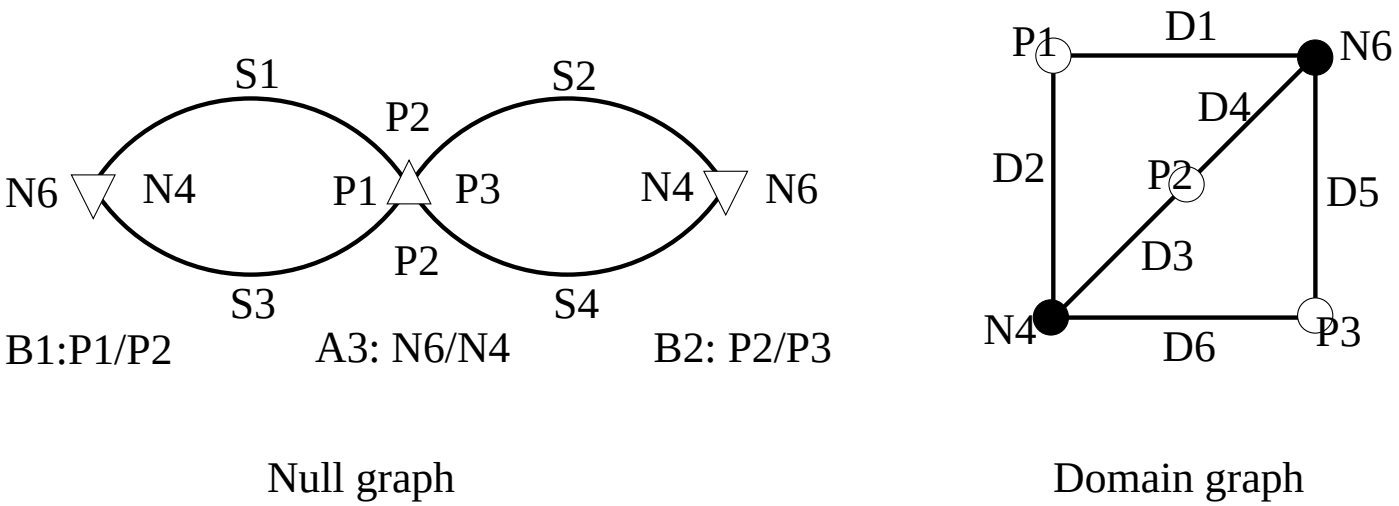


FIG. 5.—The labeled null graph (*left*) and domain graph (*right*) for the example. The vertices of the null graph are the three nulls $B_1$, $B_2$, and $A_3$ (*triangles*); its edges are the four separators, $S_1 \ldots S_4$ (*labeled*). Separators are incident on nulls in the counterclockwise order they appear from the reference spine. Between the edges are listed the sources to which the corresponding sector connects. Each null's spine sources are listed below it. The domain graph consists of six domains (edges) linking five sources vertices. The domains are labeled $\mathscr{D}_1 \ldots \mathscr{D}_6$.

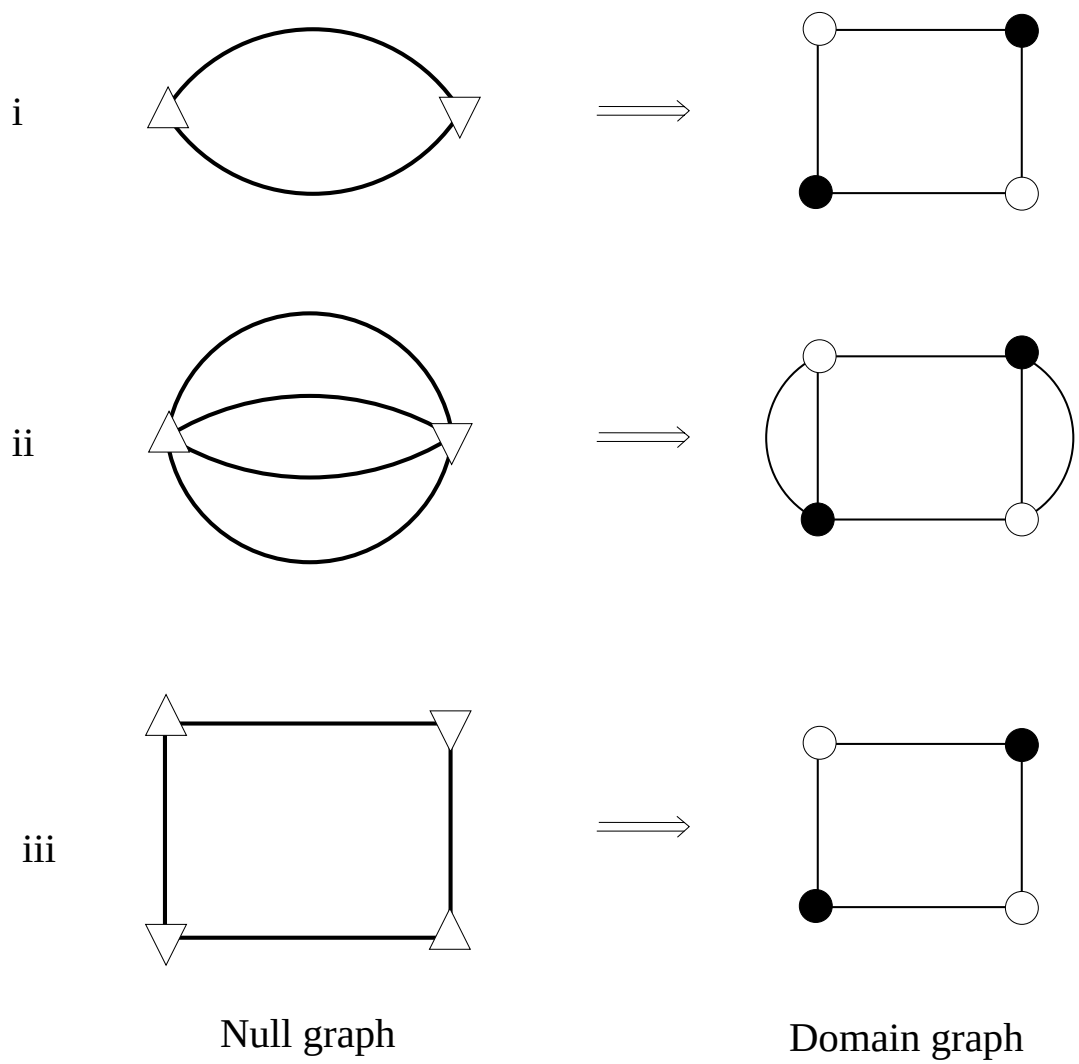


FIG. 6.—Three simple null graphs (*left*) and the domain graphs they generate (*right*)

It is possible for graph (iii) to arise from a pitchfork bifurcation of one of the nulls in graph (i). This shows that it is impossible to unambiguously deduce the structure of nulls and separators from the domain graph alone. Graph (ii) is a case where a pair of sources is connected by multiple domains. These domains cannot even be separated by a single fan, since that would be an internal null by definition. A complex example in § 6.2 shows more examples where multiple domains connect the same source pair.

## 4. QUANTIFYING THE DOMAIN FLUXES

The above procedure provides the connectivity of a potential field for any arrangement of sources. Each of the $N_d$ domains appearing in the domain graph contains a certain magnetic flux. The flux $\psi_r$ in domain $\mathscr{D}_r$ connecting $P_a$ to $N_b$ can be found by integrating $B_n$ over the region on either source skin $\partial\mathscr{R}_a$ or $\partial\mathscr{R}_b$, which intersects $\mathscr{D}_r$. (Domains will be given unique indices and denoted by the indices $r$ or $s$; thus domain $\mathscr{D}_r$ is a synonym for $\mathscr{D}_{ab}$, in a notation indicating the sources it connects.)

The domain fluxes $\psi_r$ are related to source fluxes $\Phi_a$ by the incidence matrix $M_{ar}^{(d)}$ of the domain graph (Seshu & Reed 1961; Longcope 2001)

$$\Phi_a = \sum_{r=1}^{N_d} M_{ar}^{(d)} \psi_r \ . \tag{4}$$

Element $M_{ar}^{(d)}$ of the incidence matrix is $\pm 1$ if domain $\mathscr{D}_r$ connects to source $a$, the sign of $M_{ar}^{(d)}$ being the sign of the source. Row $a$ has nonzero entries for each edge of the domain graph incident on source $a$.

We remark in passing that when one removes a subvolume enclosed by an unbroken fan that is connected to source $b$, it is also necessary to subtract flux from $\Phi_b$. In the example $\mathscr{D}_{15}$ must have flux $\psi_{15} = |\Phi_5|$. The flux of source $P_1$ must be modified $\Phi_1 \leftarrow \Phi_1 - \psi_{15}$ to reflect the removal of the domain from consideration.

### 4.1. *Chords*

Relation (4) cannot be inverted to solve for domain fluxes since the matrix has rank $N_s - 1$, because of exact flux balance, which is in general less than the $N_d$ unknowns $\psi_r$. This corresponds to the fact that fluxes within circuits of the domain graph can be varied without changing the source fluxes $\Phi_a$. It is possible to identify $N_c = N_d - N_s + 1$ domains called *chords*, whose removal from the domain graph (a process called "pruning") reduces it to a *tree*, a graph without circuits. A tree is a connected graph with $N_s - 1$ edges and a unique path connecting any pair of vertices (Seshu & Reed 1961). We will denote the chord domains $\mathscr{D}_s$, where $s = s_1, s_2, \ldots$, and use indices $i$ or $j$ for them. The set of chords $\{s_i\}_{i=1}^{N_c}$ is not unique; however, we will assume that a particular set has been selected. If the flux of every chord domain is known, then the rest of the domain fluxes may be found by solving equation (4).

The set $\{\mathscr{D}_1, \mathscr{D}_5\}$ constitute chords for the domain graph of the example (see Fig. 7). Their removal leaves a tree with four edges connecting all five sources. Alternative chord sets include $\{\mathscr{D}_2, \mathscr{D}_6\}$, $\{\mathscr{D}_1, \mathscr{D}_3\}$, and $\{\mathscr{D}_4, \mathscr{D}_5\}$.

In order to determine all domain fluxes, we must determine the fluxes of all $N_c$ chord domains. Domain $\mathscr{D}_{s_i}$ will have the general structure discussed above, enclosed by two faceted cones intersecting at a closed path of separators that we shall call $\mathscr{Q}_i$. The paths $\mathscr{Q}_1$ and $\mathscr{Q}_2$ corresponding to the chords $\mathscr{D}_1$ and $\mathscr{D}_5$ are shown on the right of Figure 7. The field lines from domain $\mathscr{D}_{s_i}$ must, in some sense, pass through $\mathscr{Q}_i$ in physical space.

To define this enclosure precisely it is necessary to exclude from the volume a set of curves that we call *flux tubes*. For each source there is one flux tube running from its source skin to infinity along a path that does not intersect any other sources or flux tubes. Once these curves are omitted from the volume, no source may be completely enclosed and a single-valued vector potential $\boldsymbol{A}(\boldsymbol{x})$ may be defined such that $\boldsymbol{B} = \nabla \times \boldsymbol{A}$. Integrating the vector potential around an infinitesimally small curve surrounding flux tube $a$ will yield

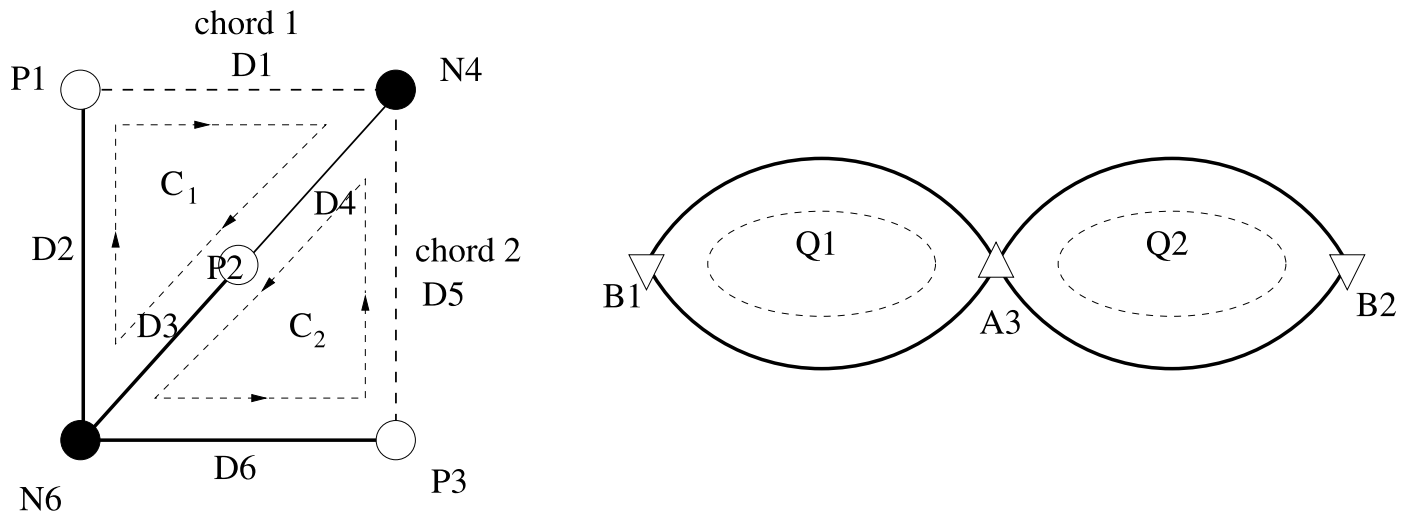


FIG. 7.—Set of chords that reduced the domain graph to a tree. The chord domains $\mathscr{D}_1$ and $\mathscr{D}_5$ are shown as dashed lines. The circuits corresponding to the chords are shown as dashed triangles, with arrows indicating their sense of orientation. The null graph on the right shows the null circuits $Q_1$ and $Q_2$ corresponding to the chords.

$\oint \boldsymbol{A} \cdot d\boldsymbol{l} = \Phi_a$, the flux of the source to which the flux tube connects.

The flux enclosed by $\mathscr{Q}_i$ may be expressed in terms of the vector potential

$$\Psi_i = \oint_{\mathscr{Q}_i} \boldsymbol{A} \cdot d\boldsymbol{l} \ . \tag{5}$$

The exact value of this integral depends on the locations of flux tubes. If the tube from source $P_a$ is deformed so that it cuts the curve $\mathscr{Q}_i$, then $\Psi_i$ will change by $\Phi_a$, the flux inside the tube.

Note that the exclusion of flux tubes makes each flux domain closed—it closes at infinity. It is therefore possible to define a *loop vector* $Q_{is}$ corresponding to loop $\mathscr{Q}_i$, where $Q_{is} = +1$ $(=-1)$ if loop $\mathscr{Q}_i$ links domain $\mathscr{D}_s$ once in the right-hand (left-hand) sense. The sense of linkage depends on the orientations of each closed curve. The domain's curve is oriented so that it goes from the positive to the negative source; the loop $\mathscr{Q}_i$ is oriented to make $Q_{is_i} = 1$ (i.e., the chord domain is positively linked). The enclosed flux can be simply written in terms of this vector:

$$\Psi_i = \boldsymbol{Q}_i \cdot \boldsymbol{\psi} = \sum_{r=1}^{N_d} Q_{ir} \psi_r \ . \tag{6}$$

Deforming a tube to cut through a path will change linkages thereby changing the vector $Q_{is}$. In particular, if the flux tube from source $a$ cuts through $\mathscr{Q}_i$, then the row-vector $\boldsymbol{Q}_i$ is changed by adding or subtracting from it row $a$ of the incidence matrix $M^{(d)}_{as}$. Because it was defined to enclose the chord domain, it is possible to define the flux tubes to make $Q_{is} = \delta_{s,s_i}$. We will henceforth assume that some definition of the flux tubes' paths has been adopted, but not necessarily this particular one.

### 4.2. *Circuit Vectors*

Suppose a removed domain $\mathscr{D}_{s_i}$ is added back to the pruned domain graph. Its return creates a unique circuit $\mathscr{C}_i$ by providing an additional connection between its endpoints; the tree provides one and only one path between any two vertices (Seshu & Reed 1961). Field lines from the domains in $\mathscr{C}_i$ form a closed path in physical space. The separator circuit $\mathscr{Q}_i$ links this closed path exactly once; $\mathscr{Q}_i$ is the *isolating loop* for circuit $\mathscr{C}_i$ in the domain graph (Longcope 2001). Figure 8 shows how the circuit $\mathscr{C}_2$ links isolating loop $\mathscr{Q}_2$ in our example.

We can define a *circuit vector* $\boldsymbol{C}^{(d)}_{si} = +1$ $(=-1)$ if domain $\mathscr{D}_s$ is traversed in the forward (backward) sense and $=0$ if $\mathscr{D}_s \notin \mathscr{C}_i$. (Each graph has a set of circuit vectors. The superscript $d$ indicates that this is a circuit vector in the domain graph.) The sense of circuit $\mathscr{C}_i$ is defined to be forward along its chord domain so that $\boldsymbol{C}^{(d)}_{s_i i} = +1$. It is evident that circuit vectors are in the null space of the incidence matrix (Seshu & Reed 1961)

$$\sum_{s=1}^{N_d} M^{(d)}_{as} C^{(d)}_{si} = 0 \ , \quad i = 1,\ 2,\ \ldots,\ N_c \ . \tag{7}$$

To see this, note that each vertex encountered by circuit $\mathscr{C}_i$ is encountered along two different edges, once in the positive and once in the negative sense.

Since the circuit $\mathscr{C}_i$ is linked once in the positive sense by the isolating loop $\mathscr{Q}_i$, then

$$\boldsymbol{Q}_i \cdot \boldsymbol{C}^{(d)}_i = \sum_{s=1}^{N_d} Q_{is} C^{(d)}_{si} = 1 \ , \quad i = 1,\ 2,\ \ldots,\ N_c \ . \tag{8}$$

Adding or subtracting rows of the incidence matrix to $Q_{is}$ will not affect this relation since the circuit vectors are orthogonal to these rows by equation (7).

Since $\mathscr{Q}_i$ encloses domain $\mathscr{D}_{s_i}$, which is in no other circuit, it links no other circuit, i.e.,

$$\boldsymbol{Q}_i \cdot \boldsymbol{C}^{(d)}_j = \delta_{ij} \ . \tag{9}$$

Expression (9) is independent of the flux-tube locations. Thus, under all deformations the vector $\boldsymbol{Q}_i$ is linearly independent of all rows in the incidence matrix and of all other vectors $\boldsymbol{Q}_j$. With fluxes defined by equation (5) and the isolating matrix $Q_{is}$ defined consistently, it is now possible to solve for the domain fluxes $\psi_s$:

$$\begin{bmatrix} M^{(d)} \\ Q \end{bmatrix} \cdot \boldsymbol{\psi} = \begin{bmatrix} \boldsymbol{\Phi} \\ \boldsymbol{\Psi} \end{bmatrix} \ . \tag{10}$$

The composite matrix is of rank $N_d$ and may be inverted provided the vector of source fluxes $\Phi_a$ sums to zero (this must be so since all columns of $M^{(d)}$ sum to zero).

### 4.3. *The Null Circuits*

The complete set of fluxes, $\Psi_i$, can be written in terms of integrals along each separator, from the positive to the neg-

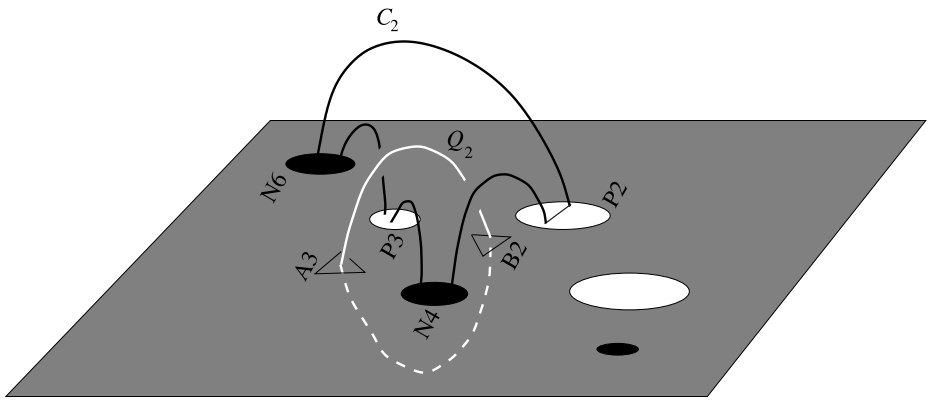


FIG. 8.—Views of the field lines in the domain circuit $\mathscr{C}_2$ (*dark curves*) and the corresponding isolating loop $\mathscr{Q}_2$ (*light curves*). The portion of $\mathscr{Q}_2$ below $z = 0$ is shown as a dashed curve.

ative null,

$$\Psi_i = \sum_{\sigma=1}^{N_{\rm nn}} C_{i\sigma}^{(o)} \int_{S_\sigma} \boldsymbol{A}\cdot d\boldsymbol{l} \ . \tag{11}$$

The matrix $C_{i\sigma}^{(o)}$ consists of circuit vectors for the null graph, defined by analogy with the circuit vectors of the domain graph. Element $C_{i\sigma}^{(o)} = 1$ $(=-1)$ if the circuit $\mathcal{Q}_i$ traces $S_\sigma$ from positive to negative null (negative to positive null), and $C_{i\sigma}^{(o)} = 0$ if $S_\sigma \notin \mathcal{Q}_i$.

The $N_c$ rows of $C_{i\sigma}^{(o)}$ are linearly independent. If they were not, it would be possible to construct a linear combination of equation (11) that summed to zero. This would mean in turn that the same linear combination of equation (6) would yield zero, in direct contradiction of equation (9).

If the null graph, with $N_{\rm nn}$ edges and $N_0$ vertices, consists of $k$ distinct components, then there are exactly $N_{\rm nn} - N_0 + k$ independent circuits, i.e., circuits whose rows are linearly independent (Seshu & Reed 1961). The number of chords in the domain graph, and therefore the number of isolating loops $\mathcal{Q}_i$, is

$$N_c = N_d - N_s + 1 = N_{\rm nn} - N_0 + 1 \ , \tag{12}$$

using equation (3) for $N_d$. It is therefore necessary that $k = 1$—the null graph must be connected. It is also necessarily true that *the set of isolating loops $\mathcal{Q}_i$ constitutes a complete set of circuits in the null graph*.

Circuit matrices, such as $C_{i\sigma}^{(o)}$, are useful in the analysis of electrical networks. Consider a network whose wires correspond to separators $S_\sigma$, with current $I_\sigma$. Kirchoff's law for these currents can be expressed in terms of the incidence matrix $M_{\beta\sigma}^{(o)}$ of the null graph

$$\sum_{\sigma=1}^{N_c} M_{\beta\sigma}^{(o)} I_\sigma = 0 \ , \quad \beta = 1,\ 2,\ \ldots,\ N_0 \ . \tag{13}$$

This means that the current vector $I_\sigma$ lives in the null space of the incidence matrix and can be expanded in terms of the circuit vectors

$$I_\sigma = \sum_{i=1}^{N_c} C_{i\sigma}^{(o)} I_i \ , \tag{14}$$

which form a basis of the null space. This relationship may be inverted

$$I_i = \sum_{\sigma=1}^{N_{\rm nn}} E_{i\sigma} I_\sigma \ , \tag{15}$$

where chords have been used to define a $E_{i\sigma}$ such that $E_{i\sigma} = C_{i\sigma}^{(o)}$ when $\sigma = \sigma_i$ and is zero otherwise.

## 5. FLUX-CONSTRAINED MINIMIZATION

The formalism developed above can be used to derive a class of nonpotential magnetic fields related to the potential field. The nonpotential fields, called flux-constrained fields, have the same domains as the potential field but with different domain fluxes. Each field is defined to minimize the magnetic energy subject to constraints on its domain fluxes. This minimization was performed in Longcope (2001) and will be described here only briefly in order to show that the construction is independent of the choice of chords.

The magnetic energy is expressed as a functional of the vector potential

$$W\{\boldsymbol{A}\} = \frac{1}{8\pi}\int |\boldsymbol{\nabla}\times\boldsymbol{A}|^2 d^3x \ . \tag{16}$$

The minimization is performed by requiring $W$ to be stationary under variations of vector potential $\boldsymbol{A}$.

Constraint functionals must be added to $W$ to ensure that the variations do not change the fluxes in any domains. The complete set of $N_d$ domain fluxes can be specified by fixing the fluxes in $N_c = N_d - N_s + 1$ isolating loops $\Psi_i$, which are defined by the set of chord domains $\{s_i\}_{i=1}^{N_c}$. The system of flux restrictions can be incorporated into a constraint functional using $N_c$ undetermined multipliers $\lambda_i$:

$$G\{\boldsymbol{A}\} \equiv \sum_i \lambda_i \left[ \sum_{\sigma=1}^{N_{\rm nn}} C_{i\sigma}^{(o)} \int_{S_\sigma} \boldsymbol{A}\cdot d\boldsymbol{l} - \sum_{s=1}^{N_d} Q_{is}\psi_s \right] . \tag{17}$$

By definition $G = 0$ for any field that satisfies all of the flux constraints, regardless of the multipliers $\lambda_i$.

It would appear that the results of this variation will depend on the choice of chord domains, since this choice enters the definition of $G$. This apparent arbitrariness may be removed by using a larger set of undetermined multipliers $\lambda_\sigma$ defined on separators and chosen to obey Kirchoff's law (13). These can be related back to the $\lambda_i$ using the matrix $E_{i\sigma}$:

$$\lambda_i = \sum_{\rho=1}^{N_{\rm nn}} E_{i\rho}\lambda_\rho \ , \quad \sum_{\rho=1}^{N_{\rm nn}} M_{\beta\rho}^{(o)}\lambda_\rho = 0 \ . \tag{18}$$

Using expression (18) in the constraint functional gives

$$G\{\boldsymbol{A}\} \equiv \sum_{\sigma=1}^{N_{\rm nn}} \lambda_\sigma \left[ \int_{S_\sigma} \boldsymbol{A}\cdot d\boldsymbol{l} - \sum_{s=1}^{N_d} \underbrace{\left( \sum_{i=1}^{N_c} E_{i\sigma} Q_{is} \right)}_{L_{\sigma s}} \psi_s \right] . \tag{19}$$

The only portion of this expression that now depends on the choice of chords is the matrix $L_{\sigma s}$, which does not affect the variation.

Expression (19) assumes that the separators $S_\sigma$ are curves, as they are in a potential field. In a more general field separatrix surfaces will intersect along a *separator ribbon* of finite width. The ribbon can be parameterized in terms of two coordinates $0 \le \eta \le 1$ and $0 \le \xi \le 1$ corresponding to its breadth and length, respectively. Defining a vector of undetermined functions $\lambda_\sigma(\eta)$ consistent with Kirchoff's law for each $\eta$ yields a constraint functional

$$G\{\boldsymbol{A}\} = \sum_{\sigma=1}^{N_{\rm nn}} \int_0^1 \lambda_\sigma(\eta) \left[ \int_0^1 \frac{\partial \boldsymbol{x}_\sigma}{\partial\xi}\cdot\boldsymbol{A}(\boldsymbol{x}) d\xi - \sum_{s=1}^{N_d} L_{\sigma s}\psi_s \right] d\eta \ , \tag{20}$$

where $\boldsymbol{x}_\sigma(\xi,\eta)$ is the ribbon surface.

The variation of the constraint functional with respect to the vector potential $\boldsymbol{A}$ provides a contribution to the current. Following Longcope (2001), this contribution is

$$\frac{\delta G}{\delta \boldsymbol{A}} = \sum_{\sigma=1}^{N_{\rm nn}} \lambda_\sigma(\eta) \left| \boldsymbol{\nabla}\xi\times\boldsymbol{\nabla}\eta \right| \frac{\partial \boldsymbol{x}_\sigma}{\partial\xi}\,\delta(S_\sigma) = \sum_{\sigma=1}^{N_{\rm nn}} \boldsymbol{J}_\sigma \ , \tag{21}$$

where $\delta(S_\sigma)$ is a Dirac $\delta$-function with support only at the separator surface. The current density $\boldsymbol{J}_\sigma$ carries a total current

$$I_\sigma = \int_0^1 \lambda_\sigma(\eta) d\eta \,, \tag{22}$$

independent of coordinate $\xi$ along the separator. The separator ribbons are thus shown to be current carriers, so it is not surprising that their undetermined multipliers must obey Kirchoff's law.

The full calculation of Longcope (2001) involves a second constraint functional to keep the field from crossing $S_\sigma$. Its contribution to the current is also localized to the separator surface. *The flux-constrained equilibrium is current-free in each magnetic domain and carries current only along separator ribbons.* The undetermined multipliers from this second functional do not contribute to the total current. A second variation with respect to the surface location $\boldsymbol{x}_\sigma(\xi, \eta)$ shows that the currents must be in weak force balance (i.e., magnetic pressure balance).

While the resulting Euler-Lagrange equation cannot be solved in practice, the arguments outlined above make clear several features of solutions that might exist. Any choice of domain chords produces an equivalent equation as we have shown by removing explicit dependence on chords. Second, every separator will be part of at least one isolating loop, regardless of chord choice, so every separator will carry some current in a general flux-constrained equilibrium. Finally, the Euler-Lagrange equation involves undetermined multipliers that generate separator current densities satisfying Kirchoff's law.

## 6. APPLICATION TO THE CORONA

The solar corona is often modeled using the potential field arising from the measured photospheric magnetic field. Observations provide the normal component of the magnetic field[3] over some patch of the solar surface. If we assume the patch to be planar, we can model the photosphere as the $z = 0$ plane, and the corona as the half-space above it ($z > 0$). The measured field, $B_z(x, y)$, is often observed to consist of concentrated flux regions surrounded by areas of much weaker magnetic field (see Fig. 9).

To construct a model of the field topology we approximate the concentrations as isolated source regions. (The procedure for making such an approximation, and its possible effect, will be treated in a subsequent work.) The boundary condition $B_z(x, y, 0) = 0$ can be satisfied without introducing additional boundaries, by using the method of images. The region $z < 0$ is included, and source skins are

[3] Often the measured component is along the line of sight, which differs from the vertical. We will not dwell on this difficulty here.

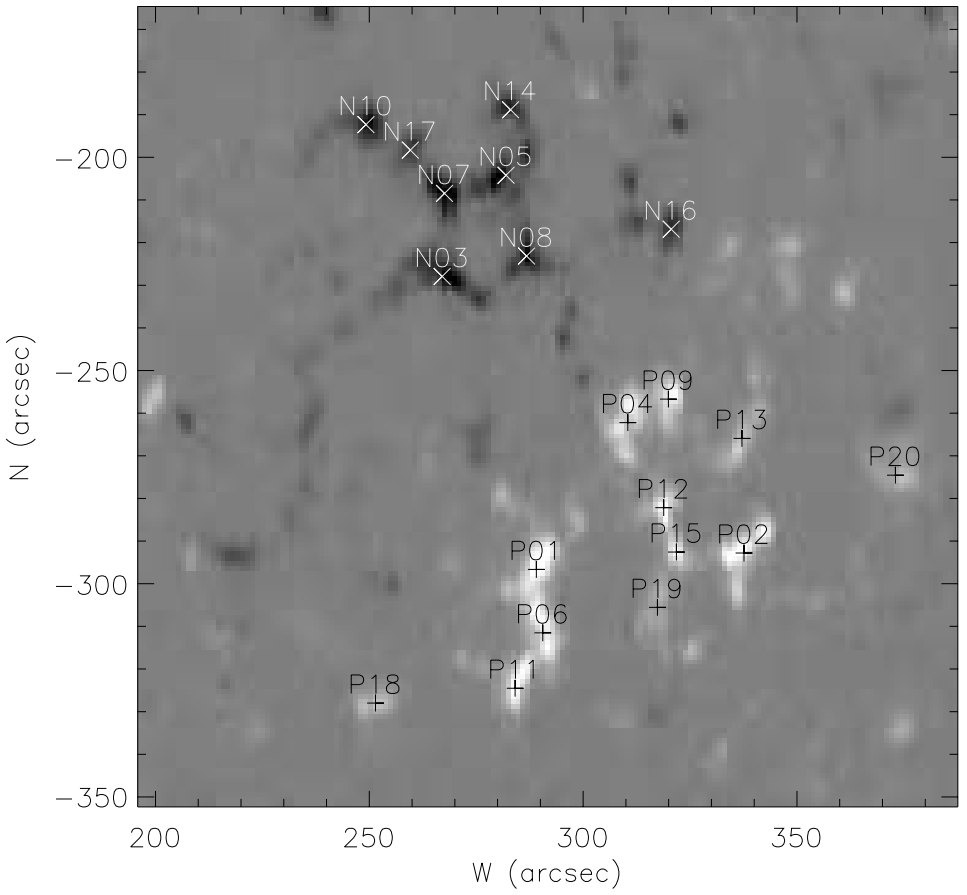


FIG. 9.—Portion of the full-disk magnetogram from Kitt Peak National Observatory on 1993 June 5. Gray scales indicate the strength of the line-of-sight magnetic field, ranging between −200 and 200 G. Labels indicate the 20 strongest flux concentrations in the field of view.

continued to the underside of each source. The normal field distribution $B_n$ is taken to be reflectionally symmetric in $z$, thus endowing the potential field with the symmetry $B_z(x, y, -z) = -B_z(x, y, z)$. Since the field is continuous outside of the sources, $B_z(x, y, 0) = 0$ there by symmetry. Whenever current is introduced in the corona, its reflection is included in the mirror corona to maintain the symmetry.

This construction satisfies the assumptions of our model provided we consider the corona as well as its mirror image, $z < 0$. The mirror corona is an artifact of the method of images and is not intended to represent the actual field below the photosphere. Our scheme above will enumerate flux domains in the mirror corona along with those in the corona. The advantage of this construction is that our general topological description need not distinguish between purely coronal domains and domains bounded by $z = 0$.

The fact that $B_z(x, y, 0) = 0$ outside the sources means that $z = 0$ is a flux surface—all field lines within it remain within it. Using the Euler characteristic, one can show (Inverarity & Priest 1999) that $N_s$ sources in the plane lead to at least $N_s - 2$ null points exactly in the plane, called *photospheric nulls*. Because of the reflectional symmetry, $\hat{z}$ is always an eigenvector of the Jacobian matrix of a photospheric null. We designate those cases where $\hat{z}$ is a spine *upright nulls* and cases where $\hat{z}$ is part of the fan *prone nulls*. Upright nulls are always internal nulls since their spines are mirror images of each other and will both go to the same source. The application of Euler characteristics to the photospheric fields states that the number of prone nulls, which we will denote $N_{p0}$, is

$$N_{p0} = N_s + N_{u0} - 2 \, , \tag{23}$$

where $N_{u0}$ are the number of upright nulls.

It is possible for nulls to appear off of the $z = 0$ plane, in symmetric pairs above and below; the former are called *coronal nulls*. If there are $N_B$ positive nulls and $N_A$ negative nulls in the volume, then the Poincaré-Hopf theorem requires (Inverarity & Priest 1999; Milnor 1965)

$$N_B - N_A = N_+ - N_- \, , \tag{24}$$

where $N_+$ and $N_-$ are the numbers of positive and negative sources. Unfortunately, there is no simple expression for the total number of nulls $N_B + N_A$ throughout the volume. If all of the photospheric nulls have been found and they do not satisfy expression (24), then there *must* be nulls off of the plane.

### 6.1. *Footprints*

It is often useful to map the magnetic domains on the photospheric plane using their *footprints*, the intersection of the domain with $z = 0$ (Welsch & Longcope 1999). Each footprint is a planar region bounded by spines and *fan traces*, curves formed from the intersections of fan surfaces with $z = 0$. Each footprint can be connected to only two sources of opposite sign, which appear as vertices of the footprint. The other footprint vertices are the photospheric nulls, including the upright nulls, which can appear as corners where three or more fan sectors meet.

The number of footprints in a map is given by an application of Euler's relation with $c = 2$ being the regions above and below the photosphere. The number of footprints is

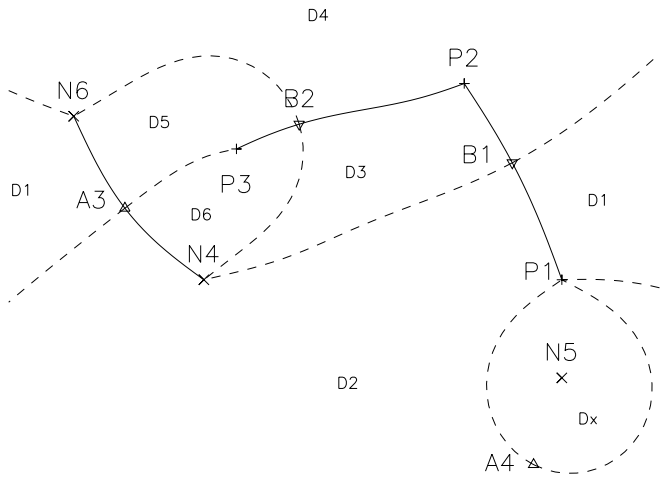


FIG. 10.—Footprint map from the example. Positive and negative sources are shown with plus signs and crosses, respectively. Positive and negative nulls are shown with downward and upward pointing triangles. Solid lines show spines, and dashed lines show fan traces. Domains are labeled, including $\mathscr{D}_x$, connecting $P_1$ to $N_5$, which forms an isolated subregion.

$f = e - v + 2$, which translates to

$$N_{\rm fp} = 3N_{p0} - N_s - N_{u0} + 2 \, , \tag{25}$$

assuming all prone nulls are part of the skeleton. This uses $e = 4N_{p0}$ since every prone photospheric null has two spines and two fan traces, all of which are edges. Using relation (23) gives the simple relationship

$$N_{\rm fp} = 2N_{p0} \, , \tag{26}$$

which is natural, since every photospheric null abuts four footprints, and every footprint must contain two nulls. The example contains six footprints, shown in Figure 10, one for each of the domains.

A purely coronal domain has no footprint and must have a counterpart in the mirror corona. Assuming that no domain has more than one footprint, the total number of domains without footprints is

$$N_d - N_{\rm fp} = N_{\rm nn} - (N_0 + 2N_{p0}) + N_s \, .$$

Using expression (23) and denoting by $N_{\rm nn}^{(c)}$ and $N_0^{(c)}$ the number of purely coronal separators and null points gives

$$N_d - N_{\rm fp} = 2(N_{\rm nn}^{(c)} - N_{p0} - N_0^{(c)} + 1) - N_{u0} \, . \tag{27}$$

The factor in parentheses is the total number of separator circuits purely in the corona. Any purely coronal domain must be encircled by a purely coronal separator circuit $\mathscr{Q}_i$.

By the symmetry of the problem the flux through a purely coronal isolating loop must match that through its mirror image. Subtracting from the total number of isolating loops, $N_c$, those strictly below the corona gives a set of

$$N_c^{(c)} = N_{\rm nn}^{(c)} - N_0^{(c)} \tag{28}$$

isolating loops whose flux may be fixed independently. Independent specification of currents on these circuits is equivalent to specifying current on each coronal separator subject to Kirchoff's law at each coronal null. To satisfy the

symmetry mirror-coronal separators must carry current opposite to their coronal image.

### 6.2. *Realistic Example*

To demonstrate the generality and power of this technique, we apply it to a complex example modeling a real active region. The magnetogram in Figure 9 shows the remnants of an active region located near disk center. Twenty flux concentrations (12 positive and eight negative) are labeled in decreasing order of their total flux, from $\Phi_1 = 1.2 \times 10^{20}$ Mx to $\Phi_{20} = 1.7 \times 10^{19}$ Mx. The collection has a net positive flux of $2.2 \times 10^{20}$ Mx (roughly 20% of the unsigned flux). This means that infinity functions as a large negative source. In spite of this large flux imbalance, we will characterize the skeleton of the potential field from this collection of sources.

To create a field model we place sources on a plane that is tangent to the solar surface at the center of unsigned flux (15°45′ south, 18°45′ west). Each source is a point whose total flux and location match that of its corresponding concentration. The potential field from this distribution has 19 null points, all photospheric and prone, in accordance with expression (23). There are 11 positive nulls, $B_1$–$B_{11}$, and eight negative nulls, $A_{12}$–$A_{19}$. The photospheric nulls therefore satisfy expression (24) where $N_+ = 12$ and $N_- = 9$ (including the negative source at infinity) so no coronal nulls are required. Nor do we find any other evidence for nulls above the $z = 0$ plane. Null $B_5$ contains the only unbroken fan, enclosing the domain connecting $P_{19}$ to infinity.

Figure 11 shows the footprints of this model field including source $P_{19}$ and null $B_5$, which are henceforth removed from consideration. The remaining $N_0 = 18$ nulls and $N_s = 20$ sources compose $N_{\rm fp} = 36$ footprints, in agreement with expression (26). Each of these is present in the map, albeit difficult to count. Null $A_{19}$ is 360 Mm to the northeast and not shown; its spines connect to $N_{10}$ and infinity.

The fan surface of each of the $N_0 = 18$ nulls was scanned to determine their fan sources and locate separators. This procedure identified $N_{\rm nn}^{(c)} = 33$ coronal separators, most of which are shown in Figure 12. Counting their mirror images

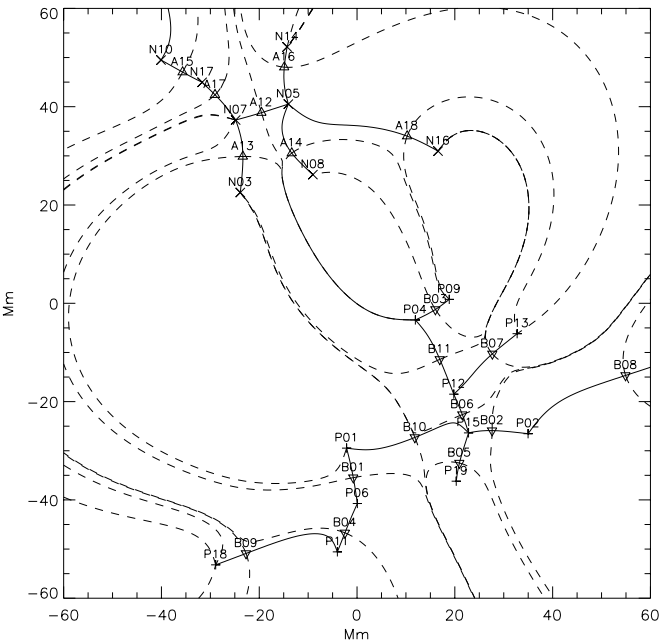


FIG. 11.—Domain footprints from 20 sources representing the magnetogram 9. Axes are in Mm from the point of tangency. Symbols are defined as in Fig. 10.

there are $N_{\rm nn} = 66$ separators in the total field. The scanning process also identified 52 pairs of connected sources, indicated in Table 1; a fan source is connected to each of the spine sources.

A list of connected pairs does not completely enumerate the domains. According to equation (3), there are $N_d = 68$ distinct domains, so many pairs are clearly connected by multiple domains. Subtracting from these the $N_{\rm fp} = 36$ footprint domains leaves 32 domains that do not intersect $z = 0$. By symmetry these must be 16 purely coronal domains and 16 mirror images. The sum of footprint and coronal domains, 52, exhausts all of the connections found in the null scan. Therefore, no pair is connected by multiple foot-

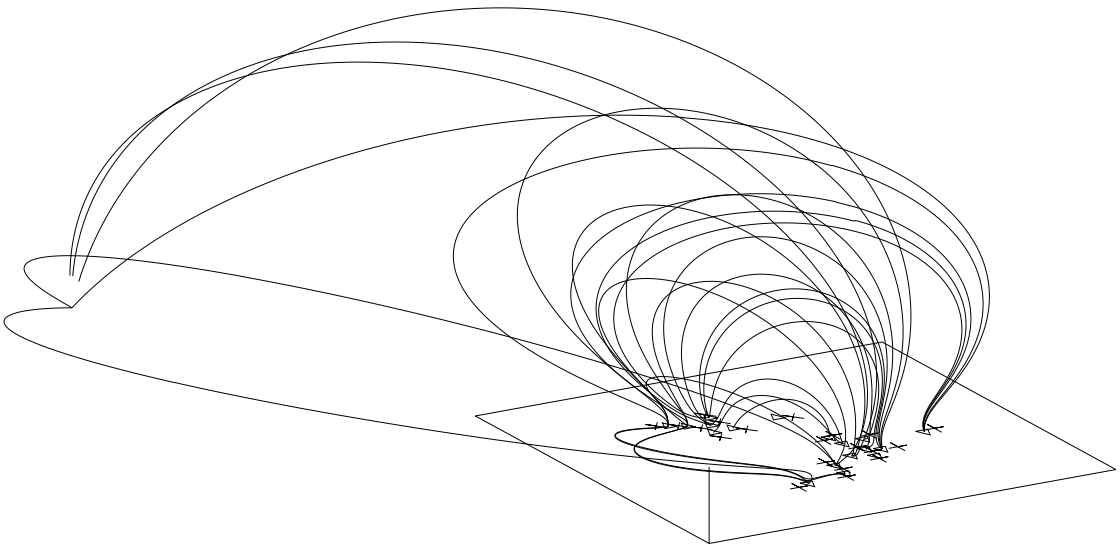

FIG. 12.—Perspective view of 28 of the 33 coronal separators

TABLE 1
THE 53 FLUX DOMAINS IN THE 20 SOURCE MAGNETIC FIELD

| | Negative Source | | | | | | | | |
|---|---|---|---|---|---|---|---|---|---|
| Positive Source | N03 | N05 | N07 | N08 | N10 | N14 | N16 | N17 | $\infty$ |
| P01 | F | * | F | * | C | * | * | C | F |
| P02 | * | C | C | * | C | F | * | C | F |
| P04 | F | F | F | F | * | * | F | * | * |
| P06 | * | * | F | * | C | * | * | C | F |
| P09 | * | F | * | F | * | * | F | * | * |
| P11 | * | * | F | * | C | * | * | C | F |
| P12 | F | C | C | * | * | F | F | * | * |
| P13 | * | F | * | * | * | F | F | * | * |
| P15 | F | C | C | * | C | F | * | C | F |
| P18 | * | * | F | * | F | * | * | F | F |
| P19 | * | * | * | * | * | * | * | * | X |
| P20 | * | F | F | * | F | F | * | F | F |

NOTE.—52 domains are found in the text plus the domain linking $P_{19}$ to $\infty$, listed with an X, which is enclosed by an unbroken fan. Domains with footprints appear as F, while purely coronal domains appear as C. Asterisks represent a lack of connection between a pair of sources.

prints or coronal domains. The sources are interconnected in roughly half of the 99 possible ways that 11 positive sources might be connected to the nine negative sources.

Each coronal domain is enclosed by one of the $N_{\rm nn}^{(c)} - N_0 + 1 = 14$ coronal separator circuits. According to expression (28) there are $N_c^{(c)} = 33$ isolating loops that may be independently constrained. Indeed, since there are no coronal nulls, a set of independent isolating loops can be formed by each coronal separator and its mirror image. The sources admit a 33-dimensional space of flux-constrained equilibria containing current sheets flowing along the 33 separators.

## 7. DISCUSSION

We have presented a general scheme for completely characterizing the connectivity of a certain class of magnetic fields. We assumed that the field is anchored in a set of discrete sources, which permits a rigorous definition of connectivity. We began with a general characterization of the skeleton of a potential magnetic field in an unbounded three-dimensional volume. The domain graph of this field followed unambiguously from its null graph. We then showed that all domain fluxes could be calculated from the integrals of the vector potential along the separators. To perform the calculation it was necessary to choose a set of chord domains for the domain graph. These correspond to a set of circuits in the null graph, known as isolating loops. Finally, we showed how the class of nonpotential fields known as flux-constrained equilibria could be generated using constraints on the fluxes through each isolating loop. This set of constraints is not unique, depending as it does on the choice of chord set. We showed, however, that the equation for the flux-constrained equilibrium did not depend on the choice of chord set and was therefore unique.

Our assumption of isolated sources is clearly an approximation to the actual solar magnetic field. Deep observations show weak vertical fields in even the quietest portions of the solar photosphere (see, e.g., Zwaan 1987). This has led several investigators to abandon the assumption and consider a continuous photospheric flux distribution $B_z(x, y, 0)$. Unfortunately, in such a continuously anchored field it is not possible to group field lines according to their terminal sources, and the field will not have separatrix surfaces of the type we have considered. It is possible to define a separatrix as the location of a discontinuity in the photospheric mapping. These are far less numerous features than the separatrices in our model; a bipolar distribution, such as Figure 9, is unlikely to have any.

Studies of continuously anchored fields have revealed features called quasiseparatrix layers (QSLs; Démoulin et al. 1996), where the mapping is continuous but severely distorted. These features can be shown to become separatrices in the limit that the photospheric flux distribution becomes discrete. The number of QSLs in a field and their location will, however, depend on the exact degree of mapping distortion defined to be "severe." This along with the need to trace every field line makes QSLs less practical as an analysis tool. Since they correspond to separatrices in a certain limit, it seems useful to work in that limit if only to simplify computations. This limit is one of discrete sources, the limit in which we have defined our model.

The set of nonpotential fields we derive are a subset of the possible flux-constrained equilibria (Longcope 2001). Our general method requires the nonpotential field to have the same connectivity as the potential field although with different amounts of flux in each domain. By setting a domain flux to zero we may effectively remove it while still satisfying the requirements of our method. Within this multidimensional space of magnetic equilibria it is possible to estimate magnetic energies in the immediate neighborhood of the potential field in terms of mutual and self-inductances (Longcope & Cowley 1996). This provides a valuable system in which to study magnetic processes such as flare energetics and magnetic reconnection.

We thank Eric Priest for useful discussions during the preparation of this manuscript and thank the anonymous referee for helpful comments. This work was supported in part by AFOSR grant F49620-00-1-0128 and in part at the Institute for Theoretical Physics, which is supported by the National Science Foundation under grant PHY99-07949.

## APPENDIX

## A BRIEF GLOSSARY OF TOPOLOGICAL TERMS

*Boundary null* (§ 3.1).—Any *null* having two distinct *spine sources* and whose fan surface is therefore a separatrix (*Antonym*: *internal null*).

*Broken fan* (§ 3.2).—A *fan surface* whose field lines connect to two or more distinct *fan sources*, which is therefore broken into *fan sectors* by separators. (*Antonym*: *unbroken fan*).

*Chord set* (§ 4.1).—A set of edges (the chords) of a graph whose removal reduces the graph to a tree.

*Circuit vector* (§ 4.2).—A column vector corresponding to one *circuit* of a graph. It has one element for each edge of the graph: $\boldsymbol{C}_{si} \neq 0$ if edge $s \in$ circuit $i$.

*Domain* (§ 2).—A continuous volume of field lines connecting a pair of sources.

*Fan sector* (§ 3.2).—A contiguous portion of a fan surface all of whose field lines end at the same *fan source*.

*Fan source* (§ 3.2).—The source lying at the other end of a fan field line from the null.

*Flux tube* (§ 4.1).—An open curve connecting a source to infinity.

*Footprint* (§ 6.1).—The two-dimensional regions formed by the intersection of a domain with the photospheric plane of reflectional symmetry $z = 0$.

*Internal null* (§ 3.1).—A null point for which both *spine sources* are the same, so its fan surface is *not* a *separatrix*. (*Antonym: boundary null*).

*Isolating loop* (§ 4.2).—A closed curve in space that links only one *domain circuit* exactly once.

*Null graph* (§ 3.3).—A schematic depiction of a field's *nulls* and *separators*.

*Photospheric null* (§ 6).—A null located within the plane of reflectional symmetry $z = 0$. (*Antonym: coronal null*).

*Prone null* (§ 6).—A *photospheric null* whose spine lies in the photosphere. (*Antonym: upright null*).

*Skeleton* (§ 2).—The collection of separatrices and separators that divides the volume into its domains.

*Source skin* (§ 2).—The closed surface surrounding a source.

*Spine source* (§ 3.1).—The source at the end of a spine opposite to the null point.

*Unbroken fan* (§ 3.2).—A fan surface for which every field line connects to the same *fan source*. (*Antonym: broken fan*).

*Upright null* (§ 6).—A *photospheric null* whose *spine* is $\hat{z}$. It is always an *internal null*. (*Antonym: prone null*).

## REFERENCES


Aulanier, G., DeLuca, E. E., Antiochos, S. K., McMullen, R. A., & Golub, L. 2000, ApJ, 540, 1126
Bagalá, L. G., Mandrini, C. H., Rovira, M. G., Démoulin, P., & Hénoux, C. H. 1995, Sol. Phys., 161, 103
Biskamp, D. 1986, Phys. Fluids, 29, 1520
Brown, D. S., & Priest, E. R. 2001, A&A, 367, 339
Bungey, T. N., Titov, V. S., & Priest, E. R. 1996, A&A, 308, 233
Démoulin, P., Hénoux, J. C., Priest, E. R., & Mandrini, C. 1996, A&A, 308, 643
Démoulin, P., Mandrini, C. H., Rovira, M. G., Hénoux, J. C., & Machado, M. E. 1994, Sol. Phys., 150, 221
Fletcher, L., Metcalf, T. R., Alexander, D., Brown, D. S., & Ryder, L. A. 2001, ApJ, 554, 451
Galsgaard, K., Priest, E. R., & Nordlund, Å. 2000, Sol. Phys., 193, 1
Gorbachev, V. S., & Somov, B. V. 1988, Sol. Phys., 117, 77
Greene, J. M. 1988, J. Geophys. Res., 93, 8583
Inverarity, G. W., & Priest, E. R. 1999, Sol. Phys., 186, 99
Lau, Y.-T., & Finn, J. M. 1990, ApJ, 350, 672
Longcope, D. W. 2001, Phys. Plasmas, 8, 5277
Longcope, D. W., & Cowley, S. C. 1996, Phys. Plasmas, 3, 2885
Longcope, D. W., & Kankelborg, C. C. 1999, ApJ, 524, 483
———. 2001, Earth, Planets and Space, 53, 571
Longcope, D. W., & Silva, A. V. R. 1998, Sol. Phys., 179, 349
Milnor, J. W. 1965, Topology From the Differentiable Viewpoint (Charlottesville: Univ. Virginia Press)
Munkres, J. R. 1984, Elements of Algebraic Topology (Redwood City: Addison-Wesley)
Parnell, C. E., Smith, J. M., Neukirch, T., & Priest, E. R. 1996, Phys. Plasmas, 3, 759
Priest, E. R., Bungey, T. N., & Titov, V. S. 1997, Geophys. Astrophys. Fluid Dyn., 84, 127
Seshu, S., & Reed, M. B. 1961, Linear Graphs and Electrical Networks (Reading: Addison-Wesley)
Sweet, P. A. 1958, Nuovo Cimento, 8, 188
Syrovatskii, S. I. 1971, Soviet Phys.–JETP, 33, 933
Welsch, B. T., & Longcope, D. W. 1999, ApJ, 522, 1117
Yeh, T. 1976, J. Geophys. Res., 81, 2140
Zwaan, C. 1987, ARA&A, 25, 83